Rapidly convergent quasi-periodic Green function throughout the spectrum—including Wood anomalies

Oscar P. Bruno* Bérangère Delourme†

March 25, 2012

Abstract

This work deals with the scattering of acoustic waves from one dimensional rough surfaces. We build a second kind integral equation that works at the Wood anomalies and is numerically efficient. The main idea is the use of a new periodic green function that quickly converges both at the Wood anomalies and away from them. We prove some theoretical results of well-posedness and we show numerical experiments that confirm the relevance of our method.

1 Introduction

This work is dedicated to the numerical simulation of periodic scattering problem. These problem has been widely investigated since it is one of great importance in applications such as optics, photonics , communications. A variety of numerical methods has been applied to periodic scattering problems, such as finite elements methods, but the method of integral equations has been widely investigated. This method has the advantageous of discretizing only the interfaces of the domain and of enforcing automatically the radiation condition. Moreover, it has been mathematically analyzed (see for instance [1],[2], [3], [4] ,[5], [6]). The construction of integral equations associated with a periodic gratings is closely related to the quasi-periodic green function. It is well known that this quasi-periodic function, defined as a series, converges extremely slowly (and cannot be directly used in a numerical method). Several methods have been investigated to increase its convergence rate: integral representations of the Green function (see [7], [8]), lattice sum method [9–13] Ewald methods (see [14],[15],[16]). An overview of these methods can be found in [14]. Recently, Monro [17] has derived an approximate green function which converges exponentially fast to the exact one. His method is based on the use of an appropriate cut off function (the main points of this method are summarized in section 3).

Nevertheless, the Wood anomaly case cannot be treated by the previous methods, since in this case the periodic Green function is even not defined. To address this difficulty, we propose a slightly different periodic green function that also converges at the Wood anomalies (4). More precisely, we provide a set of rapidly convergent periodic green functions G_j^{qp}, defined as a series that converges at least as $(1/n)^{j/2+1/2}$ when n tends toward to $\pm\infty$. Based on these new Green functions we build efficient numerical methods to solve ($\mathcal{P}$) at the Wood anomalies. The idea of using such a modified green function has already been used in [14], [18] and [19]. Compared to this previous work, our method uses rapidly converging modified

*Computing and Mathematical Sciences, Caltech, Pasadena, CA 91125
†Computing and Mathematical Sciences, Caltech, Pasadena, CA 91125

green functions, which allows us to construct efficient numerical methods. Note also that A. Barnett and L. Greengard ([20] and [21]) developed an alternative method that works at the Wood anomalies. They build a new integral equation that uses the free-space Green function alone (and not the periodic one). They force the quasi-periodic condition by adding some auxiliary layer potentials on the periodicity cell boundaries.

The remainder of this paper is organized as follows. In Section 2, we describe the scattering problem we are interested and we give some basic ideas about the quasi-periodic function and the integral equations. Section 3 deals with a windowing process that gives rise to a super-algebraically converging Green function away from Wood Anomalies. Section 4 is dedicated to the construction of new rapidly converging Green functions defined at and around Wood anomalies and their associated integral equations. Section 5 describes the numerical implementation of these new integral equations. Finally, in section 6 we show some promising numerical results.

2 Preliminaries

2.1 Scattering problem

We consider the problem of scattering of a plane wave by a perfectly reflecting periodic surface

$$\Gamma = \{(x, f(x)), x \in \mathbb{R}\}, \tag{1}$$

where $f : \mathbb{R} \mapsto \mathbb{R}$ is an L-periodic r-times continuously differentiable function (that is, $f \in \mathcal{C}^r(\mathbb{R})$) with $r \geq 2$. The incident and scattered waves propagate throughout the domain

$$\Omega = \{(x, y) \in \mathbb{R}^2, \text{such that } y > f(x)\}. \tag{2}$$

Letting $k \in \mathbb{R}^+$, $\theta \in (-\pi/2, \pi/2)$, $\alpha = k\sin(\theta)$ and $\beta = k\cos(\theta)$ (where θ is the angle between the direction of propagation of the incident field, measured counterclockwise from the negative y-axis), we assume the periodic surface is illuminated by the incident plane wave

$$u^{\text{inc}}(x, y) = e^{i(\alpha\, x - \beta y)}. \tag{3}$$

The scattered field $u^s \in H^1_{\text{loc}}(\Omega)$ is a quasi-periodic solution of the homogeneous Helmholtz equation that satisfies a radiation condition at infinity. More precisely, u^s satisfies the Partial Differential Equation (PDE)

$$\Delta u^s + k^2 u^s = 0 \quad \text{in } \Omega \tag{4}$$

as well as the quasi-periodicity condition

$$u^s(x + L, y) = u^s(x, y)e^{i\alpha L} \tag{5}$$

together with either the Dirichlet boundary conditions

$$u^s = -u^{\text{inc}} \quad \text{on } \Gamma \tag{6}$$

or the Neumann boundary conditions

$$\frac{\partial u^s}{\partial \nu} = -\frac{\partial u^{\text{inc}}}{\partial \nu} \quad \text{on } \Gamma. \tag{7}$$

Here ν is the unit normal

$$\nu(x) = \frac{-f'(x)\,\mathbf{e}_x \,+\, \mathbf{e}_y}{\sqrt{1 + f'(x)^2}} \tag{8}$$

The condition of radiation at infinity, finally, results from consideration of the Rayleigh expansion [22]

$$u^s(x,y) = \sum_{n\ in \mathbb{N}} a_n e^{i(\alpha_n x + \beta_n y)} + b_n e^{i(\alpha_n x - \beta_n y)} \quad , \quad y > H = \max_{x\in\mathbb{R}} f(x), \tag{9}$$

of the solution u^s. Here

$$\alpha_n = \alpha + \frac{nL}{k}, \quad \beta_n = \begin{cases} \sqrt{k^2 - \alpha_n^2} & \text{if } k^2 \le n^2, \\ i\sqrt{\alpha_n^2 - k^2} & \text{otherwise}. \end{cases} \tag{10}$$

We say that u^s *satisfies the condition of radiation at infinity* (or that u^s *is outgoing*) if $b_n = 0$ for all $n \in \mathbb{Z}$. In other words, u^s is outgoing if and only if u^s is given by a Rayleigh expansion of the form

$$u^s(x,y) = \sum_{n\in\mathbb{N}} a_n e^{i(\alpha_n x + \beta_n y)}, \quad y > H; \tag{11}$$

see e.g. [22].

Remark 2.1. We call U the set of integers $n \in \mathbb{Z}$ such that $\alpha_n^2 < k^2$. Note that U is a finite set. For $n \in U$, the function $e^{i(\alpha_n x + \beta_n y)}$ is an outgoing plane wave. In the case $\alpha_n^2 > k^2$, in contrast, the corresponding functions $e^{i(\alpha_n x + \beta_n y)}$ are exponentially decreasing in y: we call them surface waves. In the limiting case $\alpha_n^2 = k^2$ we have a *Wood Anomaly frequency*. In this case the function $e^{i(\alpha_n x + \beta_n y)} = e^{i(\alpha_n x)}$ is a grazing plane wave, that is, it is a plane wave that propagates parallel to the grating. We denote by $K = \{k : k = |\alpha_n|\}$ the set Wood anomaly frequencies.

We have the following results of well-posedness:

Theorem 2.2. *The Dirichlet problem is well posed for all values of the frequency $k > 0$, that is, for all $k > 0$ there exists one and only one function $u^s \in H^1_{loc}(\Omega)$ which satisfies the Helmholtz equation (4) together with the Dirichlet condition (6), the quasi-periodicity condition (5) and the radiation condition (11). The Neumann problem (4, 7, 5, 11) is well posed except for a discrete set of frequencies k that accumulates only at infinity.*

Proofs of these results can be found in references [22–25].

2.2 Classical quasi-periodic Green function

Let $k \notin K$ (k is not a Wood anomaly) and let $(X,Y) \in \mathbb{R}^2$. The quasi-Periodic Green function G^{q} is defined by

$$G^{\mathrm{q}}(X,Y) = \sum_{n\in\mathbb{Z}} e^{-i\alpha nL} G(X + nL, Y). \tag{12}$$

where G is the Green function of $\mathbb{R}^2$, defined for $(X,Y) \neq (0,0)$

$$G(X,Y) = \frac{i}{4} H_0^1(k\sqrt{X^2+Y^2}). \tag{13}$$

As is known, the series (12) converges for $(X,Y) \neq (Ln, 0)$, $n \in \mathbb{Z}$. Further, the truncated series

$$G^{\mathrm{q}}(X,Y) = \sum_{n\in\mathbb{Z}, |n|\ge 2} e^{-i\alpha nL} G(X + nL, Y)$$

converges uniformly in any compact set not containing singularities of G^{q} (see e.g. theorem 4.1 in [6]). For reference, finally, we note that the Green function also admits the Rayleigh expansion

$$G^{\mathrm{q}}(X,Y) = \sum_{n\in\mathbb{Z}} \frac{i}{2L} \frac{e^{i\alpha_n X + i\beta_n |Y|}}{\beta_n} \tag{14}$$

(see e.g. theorem 4.4 in [6]).

2.3 Integral equation formulations

Here and in what follows we denote by $\Omega_\#$ and $\Gamma_\#$ the intersection of Ω and Γ, respectively, with the set $x \in (-\frac{L}{2}, \frac{L}{2}) \times \mathbb{R}$:

$$\Omega_\# = \left\{ (x,y) \in \left(-\frac{L}{2}, \frac{L}{2}\right) \times \mathbb{R}, \text{ such that } y > f(x) \right\} \quad , \quad \Gamma_\# = \left\{ (x, f(x)), x \in \left(-\frac{L}{2}, \frac{L}{2}\right) \right\}. \tag{15}$$

As is well known, the scattering problems described in Section 2.1 can be reduced to second kind integral equations (cf. for instance [22, 23]). For simplicity and definiteness, in this paper we consider the following integral formulations of the Dirichlet and Neumann problems.

$$-u^{\mathrm{inc}}{}_{|\Gamma_\#} = \int_{\Gamma_\#} \partial_{\nu(x')} G^{\mathrm{q}} \left(x - x', f(x) - f(x')\right) \mu(x')\, ds(x') + \frac{1}{2}\mu(x'),$$

The diffracted field is then obtained by a post-processing step using the following representation formula:

$$u^s(x,y) = \int_{\Gamma_\#} \partial_{\nu(x')} G^{\mathrm{q}} \left(x - x', y - f(x')\right) \mu(x')\, ds(x').$$

For the Neumann problem, we shall also solve a second kind integral equation: find μ continuous and α-quasiperiodic such that

$$-\partial_{\nu(x)} u^{\mathrm{inc}}{}_{|\Gamma_\#} = \int_{\Gamma_\#} \partial_{\nu(x)} G^{\mathrm{q}} \left(x - x', f(x) - f(x')\right) \mu(x')\, ds(x') - \frac{1}{2}\mu(x'),$$

and the diffracted field will be obtained by a slightly different representation formula:

$$u^s(x,y) = \int_{\Gamma_\#} G^{\mathrm{q}} \left(x - x', y - f(x')\right) \mu(x')\, ds(x').$$

3 Superalgebraically convergent representation away from Wood anomalies

In this section we describe an efficient methodology, put forth in [17], for evaluation of the quasi-periodic Green function. Although only applicable away from Wood anomalies, the basic idea in this method, namely, smooth windowing, is incorporated as part of our overall all-frequency scheme for additional efficiency at non-Wood anomaly frequencies, and for ease of implementation of high-order Nyström methods. The algorithm [17] is based on a certain smooth truncation of the series (12) defining the Green function. As established in that reference and demonstrated in a simple example in what follows, integrals involving such smoothly truncated Green function converge exponentially fast to the corresponding integrals involving the exact periodic Green function.

To introduce this algorithm, let us consider the smooth cut-off function

$$S(x,x_0,x_1)=\begin{cases}1 & \text{if } |x|\le x_0,\\ \exp\left(\frac{2e^{-1/u}}{u-1}\right) & \text{if } x_0<|x|<x_1, \quad u=\frac{|x|-x_0}{x_1-x_0},\\ 0 & \text{if } |x|\ge x_1,\end{cases} \tag{16}$$

and let us define the approximate periodic Green function G^{q}_A by

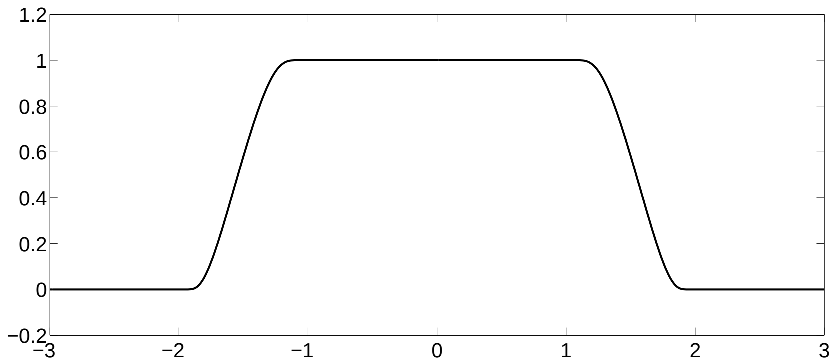

Figure 1: Function S, for $x_0=1$, $x_1=2$

$$G^{\mathrm{q}}_A(X,Y)=\frac{i}{4}\sum_{n\in\mathbb{Z}}e^{-i\alpha nL}\,S(X+nL,cA,A)\,H^1_0(k\sqrt{(X+nL)^2+(Y)^2}) \tag{17}$$

and

$$H^{\mathrm{q}}_A(x,x')=\frac{i}{4}\sum_{n\in\mathbb{Z}}e^{-i\alpha nL}\,S(x-x'+nL,cA,A)\,\partial_{\nu(x')}H^1_0(k\sqrt{(x-x'+nL)^2+(y-y')^2}) \tag{18}$$

where $A>L$ and $0<c<1$. Then the following result holds:

Theorem 3.1. *Let $k\notin K$ and let f be a smooth function. Then, for any α-quasi-periodic smooth function μ the integral*

$$\int_{\Gamma_\#}H^{\mathrm{q}}_A(x,x')\,\mu(x')ds(x') \quad \textit{and} \quad \int_{\Gamma_\#}G^{\mathrm{q}}_A(x-x',f(x)-f(x'))\,\mu(x')ds(x')$$

respectivelly converge superalgebraically fast (that is, faster than any power to $1/A$) to

$$\int_{\Gamma_\#}\partial_{\nu(x')}G^{\mathrm{q}}(x-x',f(x)-f(x'))\,\mu(x')ds(x') \quad \textit{and} \quad \int_{\Gamma_\#}G^{\mathrm{q}}(x-x',f(x)-f(x'))\,\mu(x')ds(x')$$

as A tends to infinity.

The main idea of the proof of this result can be conveyed by a simplified example (that results from consideration of the asymptotics of the Hankel function) which we present in what follows; cf. reference [17] which also contains a proof of Theorem 3.1.

For definiteness we consider the case of double-layer potential only; the case of the single layer is even more direct. Since μ is α-quasiperiodic the double layer potential can be expressed in the form

$$\int_{\Gamma_\#} \partial_{\nu(x')} G^{\mathrm{q}}\left(x - x', f(x) - f(x')\right)\, \mu(x') ds(x')$$
$$= \int_{-\infty}^{\infty} \partial_{\nu(x')} G\left(x - x', f(x) - f(x')\right)\, \mu(x') \sqrt{1 + f'(x')^2}\, dx'. \quad (19)$$

Taking into account the large z asymptotic behavior of the Hankel function $H_1^1(z)$, $H_1^1(z) \sim C\frac{e^{iz}}{\sqrt{z}}$, for large positive values of x' we obtain

$$\partial_{\nu(x')} G\left(x - x', f(x) - f(x')\right) \sim C(x, x')\frac{e^{ikx'}}{\sqrt{x'}}, \quad (20)$$

where C is a smooth bounded function. On the other hand $\mu(x')\sqrt{1 + f'(x')^2}$ is an α-quasiperiodic function, and it can therefore be expanded in a Rayleigh series of the form $\sum_{n=-\infty}^{\infty} a_n e^{i\alpha_n x'}$. In our simplified example we replace the Green function by the asymptotic form (20) with $C(x, x') = 1$, so that the integrand equals an infinite sum of terms of the form $\frac{e^{ik_n x}}{\sqrt{x}}$ (where $k_n = k - \alpha - \dfrac{2\pi n}{L}$). And, in fact, for our example we consider just one such term, that is, we study the integration problem

$$I_{\text{ex}} = \int_0^{+\infty} \frac{e^{ik_n x'}}{\sqrt{x'}}\, dx'.$$

As stated above, throughout this section we assume k is not a Wood anomaly frequency ($k \notin K$), or, in other words, $k_n \neq 0$ for all n.

A	$\lvert I_{\text{ex}} - I^A_{\text{per}}\rvert$	$\lvert I_{\text{ex}} - I_{S,A}\rvert$
10	5.0×10^{-2}	8.5×10^{-5}
20	3.6×10^{-2}	9.7×10^{-7}
25	3.2×10^{-2}	1.9×10^{-7}
50	2.3×10^{-2}	4.9×10^{-10}
75	1.8×10^{-2}	4.7×10^{-11}
100	1.6×10^{-2}	7.7×10^{-14}

Table 1: Approximation errors for various A ($k_n = 2\pi c = 0.1$)

To illustrate Theorem 3.1 in the present context we investigate theoretically and numerically the convergence of the approximation

$$I_{S,A} = \int_0^{+\infty} S(x', cA, A)\, \frac{e^{ik_n x'}}{\sqrt{x'}}\, dx'$$

to the exact value I_{ex}. For comparison purposes we also consider the classical approximation

$$I_{H,A} = \int_0^{A} \frac{e^{ik_n x'}}{\sqrt{x'}}\, dx', \quad (21)$$

which can be viewed as the result of substituting the smooth windowing function S by a suitable Heaviside function H, and which corresponds, in the context of this section, to the direct truncation of the series (12) keeping $\mathcal{O}(A/L)$ terms. The error $I_{\text{ex}} - I_{S,A}$ in the windowed approximation is given by

$$I_{\text{ex}} - I_{S,A} \; = \; \int_0^{+\infty} (1 - S(x', cA, A)) \, \frac{e^{ik_n x'}}{\sqrt{x'}} \, dx' \; = \; \int_{cA}^{+\infty} P(x', cA, A) \, \frac{e^{ik_n x'}}{\sqrt{x'}} \, dx',$$

where $P(x', c, A) = 1 - S(x', cA, A)$. Using the the change of variables $x = \frac{x'}{ca}$ we obtain

$$I_{\text{ex}} - I_{S,A} = \sqrt{cA} \int_1^{+\infty} \frac{P(x, 1, \frac{1}{c})}{\sqrt{x}} \, e^{ik_n cAx} \, dx.$$

Given that $P(1, 1, \frac{1}{c}) = 0$, integration by parts once yields

$$I_{\text{ex}} - I_{S,A} = -\frac{1}{ik_n \sqrt{cA}} \int_1^{+\infty} \frac{\partial}{\partial x} \left(\frac{P(x, 1, \frac{1}{c})}{\sqrt{x}} \right) e^{ik_n cAx} \, dx,$$

while, more generally, p-times iterated integration by parts gives rise to the relation

$$I_{\text{ex}} - I_{S,A} = \frac{(-1)^p}{(ik_n)^p (cA)^{p-1/2}} \int_1^{+\infty} \frac{\partial^p}{\partial x^p} \left(\frac{P(x, 1, \frac{1}{c})}{\sqrt{x}} \right) e^{ik_n cAx} \, dx.$$

Noting that the derivatives of $\frac{P(x,1,\frac{1}{c})}{\sqrt{x}}$ do not depend on A, and are bounded functions with support equal to the interval $[1, 1/c]$, for all $p \in \mathbb{N}$ we obtain

$$|I_{\text{ex}} - I_{S,A}| \leq \frac{C}{\sqrt{k_n} \, (k_n \, c \, A)^{p-1/2}}.$$

In other words, the error in the windowed approximation $I_{S,A}$ is superalgebraically small: it is a quantity of order A^{-p} for all $p \geq 1$.

The widowed integration method thus results in much closer approximations than the direct un-windowed approximation $I_{H,A}$: a simple argument involving a single integration by parts shows that the error in the latter approximation decays like $A^{-\frac{1}{2}}$. Table 3 illustrates the superalgebraically fast convergence of $I_{S,A}$ as well as the extremely slow convergence of $I_{H,A}$.

4 New, rapidly convergent quasi-periodic Green functions series valid at and around Wood anomalies

4.1 New quasi-periodic Green function: introduction

We seek a quasi-periodic Green function $\tilde{G}_j^{\text{q}}$ that can be expressed by a rapidly-convergent series

$$\tilde{G}_j^{\text{q}}(X, Y) = \sum_{n=-\infty}^{\infty} e^{-i\alpha nL} G_j(X + nL, Y), \tag{22}$$

($j \in \mathbb{N}$), where $G_j(X, Y)$ is a certain j-dependent half space Green function defined in Section 4.2, which decays rapidly as X tends to infinity. As a result of this fast decay, a truncated sum of the form

$$\tilde{G}_j^N(X, Y) = \sum_{|n| \leq N-1} e^{-i\alpha nL} G_j(X + nL, Y) \tag{23}$$

converges more rapidly than does a corresponding truncation of the classical quasi-periodic Green function (12): for $Y \in (-M, M)$ there exists a constant $C > 0$, such that for all $X \in (-L, L)^2$ we have

$$\left|\tilde{G}^{\mathrm{q}}_j(X,Y) - \tilde{G}^{N}_j(X,Y)\right| \leq \begin{cases} \dfrac{C}{N^{\frac{j-1}{2}}} & \text{if } n \text{ even} \\ \dfrac{C}{N^{\frac{j}{2}}} & \text{if } n \text{ odd} \end{cases}$$

In particular, the series expansion (22) for the new Green function converges rapidly for all frequencies k, even at and around Wood anomaly frequencies.

Remark 4.1. Our proposed rapidly convergent quasi-periodic Green function series, which is denoted by G^{q}_j, results from a slight but important modification of $\tilde{G}^{\mathrm{q}}_j$; see Section 4.4 for details.

4.2 Rapidly decaying (non-periodic) half-space Green function

To introduce our rapidly decaying half space Green function we rely on differences of values of the free-space Green function and ideas related to the method of images. Indeed, using the mean value theorem, we see that there exists a real value of ξ, $Y < \xi < Y + h$, such that

$$H^1_0\left(k\sqrt{X^2+Y^2}\right) - H^1_0\left(k\sqrt{X^2+(Y+h)^2}\right) = \frac{h\,k(Y+\xi)}{\sqrt{X^2+(Y+\xi)^2}} H^1_1\left(k\sqrt{X^2+(Y+\xi)^2}\right) \quad (24)$$

Thus, in view of the asymptotic formula

$$H^1_n(t) = \sqrt{\frac{2}{\pi t}} e^{i\left(t - n\frac{\pi}{2} - \frac{\pi}{4}\right)} \left\{1 + O\left(\frac{1}{t}\right)\right\}, \quad t \in \mathbb{R},\ n \in \mathbb{N}_0 \quad (25)$$

there exists a constant $C > 0$ such that, for large $|X|$ we have

$$\left|H^1_0\left(k\sqrt{X^2+Y^2}\right) - H^1_0\left(k\sqrt{X^2+(Y+h)^2}\right)\right| \leq \frac{C}{|X|^{3/2}}. \quad (26)$$

That is, the expression on the left hand side of equation (24), which is a Green function in the domain $Y > -h$, decays faster, as $X \to \infty$ than the free space Green function (13).

Green functions with arbitrarily fast algebraic decay can be obtained by generalizing the previous idea, using a finite-difference operator that approximates a higher-order Y-derivative operator, instead of the difference shown on the left hand side of equation (24). In this paper we use the finite-difference operator

$$(u_\ell)_{\ell=0}^{j} \to \sum_{\ell=0}^{j} (-1)^\ell\, C^\ell_j\, u_\ell, \quad (27)$$

where C^l_j denote the binomial coefficients $C^l_j = \dfrac{l!}{j!(j-l)!}$. As is known, the operator (27) differentiates exactly polynomials of degree $< j$: for all polynomials $P(Z) = \sum_{\ell}^{j-1} a_\ell Z^\ell$ we have

$$\sum_{\ell=0}^{j} (-1)^\ell\, C^\ell_j\, P(Z + \varepsilon\ell) = 0, \quad (28)$$

Using a Taylor expansion it thus follows that, for a smooth function v we have

$$\sum_{\ell=0}^{j}(-1)^{\ell}\, C_j^{\ell}\, v(Z+\varepsilon\ell) = \varepsilon^j \sum_{\ell=1}^{j} C_j^{\ell}\,(-1)^{\ell}\,\frac{\ell^j}{j!} v^{(j)}(Z+\xi_\ell), \quad 0\le \xi_\ell \le \varepsilon\,\ell; \tag{29}$$

Letting $h>0$ and $j\in\mathbb{N}$, and, for $(X,Y)\neq(0,lh)$, $l\in\mathbb{N}$, $l\le j$, we thus define the j-th rapidly-decaying half-space Green function by

$$G_j(X,Y) = \frac{i}{4}\sum_{\ell=0}^{j}\,(-1)^{\ell}\,C_j^{\ell}\,H_0^1\left(k\sqrt{X^2+(Y\,+\,\ell\,h)^2}\right). \tag{30}$$

The corresponding quasi-periodic Green function (22) can thus be expressed in the

$$\tilde{G}_j^{\mathrm{q}}(X,Y) = \frac{i}{4}\sum_{n=-\infty}^{\infty} e^{-i\alpha nL}\sum_{\ell=0}^{j}\,(-1)^{\ell}\,C_j^{\ell}\,H_0^1\left(k\sqrt{(X+nL)^2+(Y\,+\,\ell\,h)^2}\right) \tag{31}$$

G_j does indeed decay rapidly, as shown in Lemma 4.2;

Lemma 4.2. *Let $j\in\mathbb{N}$. Then, for each $k>0$, $h>0$ and $M>0$ there exists a positive constant C (that depends on k, h and M) such that, for all $Y\in(-M,M)$ and for all real numbers X with $|X|>1$ we have*

$$|G_j(X,Y)| \;\le\; \begin{cases} \dfrac{C}{|X|^{\frac{j+1}{2}}} & \text{if } j \text{ even},\\[2ex] \dfrac{C}{|X|^{\frac{j+1}{2}+\frac{1}{2}}} & \text{if } j \text{ odd}. \end{cases} \tag{32}$$

Proof. Let

$$f(Z;X) = \frac{i}{4}H_1^0\left(k\,|X|u(Z)\right), \qquad u(Z)=\sqrt{1+Z^2}; \tag{33}$$

Since, as it is easily seen we have

$$G_j(X,Y) = \sum_{\ell=0}^{j}\,C_j^{\ell}\,(-1)^{\ell}\,f\Big(\,\frac{Y}{|X|}+\frac{\ell h}{|X|}\,;X\Big),$$

to study the decay rate of $G_j(X,Y)$ as $X\to\infty$ we apply the relation (29) to the function $v(Z)=f(Z;X)$, with fixed values of X, at the point $Z=\frac{Y}{X}$ and $\varepsilon=\frac{h}{|X|}$. We thus obtain

$$G_j(X,Y) = \sum_{\ell=1}^{j}\left(\frac{h}{X}\right)^j\,\frac{C_j^{\ell}\,(-1)^{\ell}\ell^j}{j!}\,f^{(j)}\Big(\,\frac{Y}{|X|}+\xi_\ell\,;X\Big)\quad 0\le\xi_\ell\le\frac{\ell h}{|X|}. \tag{34}$$

To complete the proof we estimate the quantity $\left|f^{(j)}\Big(\frac{Y}{|X|}+\xi_\ell\,;\,X\Big)\right|$, for $\ell<j$. To do this we use Faá di Bruno's formula []

$$\begin{aligned} f^{(n)}(Z\,;X) \;&=\; \frac{i}{4}\,\frac{d^n}{dZ^n}\left(H_0^1\big(k\,|X|\,u(Z)\big)\right),\\ &=\; \frac{i}{4}\,\sum\;\frac{n!}{\prod_{q=1}^{n}(m_q!)(q!)^{m_q}}\;(H_0^1)^{(\sum_{q=1}^{n}m_q)}\big(k\,|X|\,u(Z)\big)\;\prod_{q=1}^{n}\Big(k\,|X|\,u^{(q)}(Z)\Big)^{m_q}, \end{aligned}$$

where the sum is taken over all n-tuples $(m_1, m_2, \cdots, m_n)$ satisfying $\sum_{q=1}^n q\, m_q = n$. Note that, as is easily shown,

$$\sum_{q=1}^{n/2} m_{2q} \leq \frac{n}{2} \quad \text{if } n \text{ is even,} \tag{35}$$

and

$$\sum_{q=1}^{(n-1)/2} m_{2q} \leq \frac{n-1}{2} \quad \text{if } n \text{ is odd.} \tag{36}$$

We estimate in turn $(H_0^1)^{(\sum_{q=1}^n m_q)} \left(k\,|X|\,u\left(\frac{Y}{|X|} + \xi_\ell\right)\right)$ and $\prod_{q=1}^n \left(k\,|X|\,u^{(q)}\left(\frac{Y}{|X|} + \xi_\ell\right)\right)^{m_q}$, $\xi_\ell \leq \frac{\ell h}{|X|}$. Using Hankel function derivative formulas (cf [26]), it is easily seen that there exists constants $c_{p,q}$ such that

$$(H_0^1)^{(p)}\big(k\,|X|\,u(Z)\big) = \sum_{q=0}^{p} c_{q,p}\, H_q^1\big(k\,|X|\,u(Z)\big).$$

Consequently, since $|H_q^1(t)| \leq \frac{C}{t^{1/2}}$ and since $\left|\frac{Y}{|X|} + \xi_\ell\right| \leq \frac{C}{|X|}$, we obtain

$$\left|(H_0^1)^{(p)}\left(k\,|x-x'|\,u\left(\frac{Y}{|X|} + \xi_\ell\right)\right)\right| \leq \frac{C}{|X|^{1/2}}. \tag{37}$$

Note that C might depend on k, M and l. To estimate $\prod_{q=1}^n \left(k\,|X|\,u^{(q)}\left(\frac{Y}{|X|} + \xi_\ell\right)\right)^{m_q}$ we first remark that, for small Z,

$$u^{(q)}(X) \leq \begin{cases} C & \text{if } q \text{ is even,} \\ C\,Z & \text{if } q \text{ is odd.} \end{cases} \tag{38}$$

It follows that

$$\prod_{q=1}^n \left(k\,|X|\,u^{(q)}\left(\frac{Y}{|X|} + \xi_\ell\right)\right)^{m_q} \leq \begin{cases} C\,|X|^{\sum_{q=1}^n m_q - \sum_{q=1}^{n/2} m_{2q-1}} \leq C\,|X|^{\sum_{q=1}^{n/2} m_{2q}} & n \text{ is even,} \\ C\,|X|^{\sum_{q=1}^n m_q - \sum_{q=1}^{(n+1)/2} m_{2q-1}} \leq C\,|X|^{\sum_{q=1}^{(n-1)/2} m_{2q}} & n \text{ is odd.} \end{cases} \tag{39}$$

Thus, using formulas (35) and (36), we obtain

$$\prod_{q=1}^n \left(k\,|X|\,u^{(q)}\left(\frac{Y}{|X|} + \xi_\ell\right)\right)^{m_q} \leq \begin{cases} C\,|X|^{\frac{n}{2}} & \text{if } n \text{ is even,} \\ C\,|X|^{\frac{n-1}{2}} & \text{if } n \text{ is odd.} \end{cases} \tag{40}$$

Combining (37) and (40) we obtain

$$\left|f^{(n)}\left(\frac{Y}{|X|} + \xi_\ell\,; X\right)\right| \leq \begin{cases} C\,|X|^{\frac{n}{2}-\frac{1}{2}} & \text{if } n \text{ is even,} \\ C\,|X|^{\frac{n}{2}-1} & \text{if } n \text{ is odd.} \end{cases} \tag{41}$$

Finally, the result of Lemma 4.2 directly follows from (44) and (41):

$$|G_j(X,Y)| \leq \begin{cases} C\,\dfrac{1}{|X|^{j-(\frac{j}{2}-\frac{1}{2})}} & \text{if } n \text{ is even,} \\[2ex] C\,\dfrac{1}{|X|^{j-(\frac{j}{2}-1)}} & \text{if } n \text{ is odd.} \end{cases} \tag{42}$$

$\square$

As may be expected, the normal derivatives of the Green functions G_j (which are needed in the integral formulations laid down in Section 2.3) also decay rapidly at infinity. The details are presented in the following theorem.

Lemma 4.3. *Let $j \in \mathbb{N}^*$. Then, for each $k > 0$, $h > 0$, $M > 0$, and $f \in \mathcal{C}^2(\Gamma)$, there exists a positive constant C, such that , for all $x \in \left(-\frac{L}{2}, \frac{L}{2}\right)$, for all $y \in (-M, M)$, for all real number x' with $|x'| > 1$ we have,*

$$\left|\frac{\partial G_j}{\partial \nu(x')}(x - x', y - f(x'))\right| \le \begin{cases} \dfrac{C}{|x - x'|^{j/2+1/2}} & \text{if } j \text{ even}, \\ \dfrac{C}{|x - x'|^{(j+1)/2+1/2}} & \text{if } j \text{ odd}. \end{cases} \tag{43}$$

Proof. The proof is similar to the proof of Lemma 4.4. We first introduce the function $g(z, x - x')$

$$g(z; x - x') = \frac{k\left(z|x - x'| - (x - x')f'(x')\right)}{|x - x'|\sqrt{1 + z^2}} H_1^1\left(k|x - x'|\sqrt{1 + z^2}\right),$$

and we remark that

$$\frac{\partial G_j}{\partial \nu(x')}(x - x', y - f(x')) = \sum_{\ell=0}^{j} (-1)^\ell \, C_\ell^j \, g(z + \ell\varepsilon; x - x')$$

at the point $z = \frac{y - f(x')}{x - x'}$ and $\varepsilon = \frac{h}{|x - x'|}$. Using the finite difference formula (29), we thus obtain

$$\frac{\partial G_j}{\partial \nu(x')}(x - x', y - f(x')) = \sum_{\ell=1}^{j} \left(\frac{h}{X}\right)^j \frac{C_j^\ell \, (-1)^\ell \ell^j}{j!} \, g^{(j)}\left(\frac{y - f(x')}{|x - x'|} + \xi_\ell \, ; x - x'\right) \quad 0 \le \xi_\ell \le \frac{\ell h}{|x - x'|}. \tag{44}$$

The proof is completed by estimating the quantity $g^{(j)}\left(\frac{y - f(x')}{|x - x'|} + \xi_\ell \, ; x - x'\right)$, as it is done is the proof of Lemma 4.4

□

4.3 Fast convergence of the quasi-periodic Green function series (22)

In view of the results of Section 4.2 it is easy to verify that the series in equation (22) and its term-by-term normal derivative converge rapidly (that is, that the tails of the series converge rapidly to zero), as detailed in the following theorem.

Theorem 4.4. *Let $j \in \mathbb{N}$, $N \in \mathbb{N}$, $h > 0$ and $M > 0$. Then, there exists a constant $C_1 > 0$ such that, for all x, x', y and y' satisfying*

1. $-\frac{L}{2} < x < \frac{L}{2}$, $-\frac{L}{2} < x' < \frac{L}{2}$,
2. $-M < y < M$, $-M < y' < M$, *and*
3. $(x - x', y - y') \ne (nL, -\ell h)$ *for any pair* $(n, \ell) \in \mathbb{Z}^2$ *with* $0 \le \ell \le j$,

we have

$$\left|\sum_{n \in \mathbb{Z}, |n| \ge N} e^{-i\alpha_n L} G_j\left(x - x' + nL, y - y'\right)\right| \le \begin{cases} \dfrac{C_1}{N^{j/2-1/2}} & \text{if } j \text{ is even}, \\ \dfrac{C_1}{N^{j/2}} & \text{if } j \text{ is odd}. \end{cases}$$

In other words, the quasi-periodic Green function series (22), (30) *with j even (resp. j odd) converges with an algebraically small error of order $(j-1)/2$ (resp. $j/2$).*

Similarly, there exists a constant $C_2 > 0$ such that, for all x, x', y and y' satisfying points 1. and 3. above, as well as $-M < y < M$, we have

$$\left|\sum_{n\in\mathbb{Z},|n|\geq N+1} e^{-i\alpha_n L}\frac{\partial G_j}{\partial\nu(x')}\left(x-x'+nL, y-f(x')\right)\right| \leq \begin{cases} \dfrac{C_2}{N^{j/2-1/2}} & \text{if } j \text{ is even,} \\ \dfrac{C_2}{N^{j/2}} & \text{if } j \text{ is odd.} \end{cases}$$

That is to say, the termwise normal derivative of the quasi-periodic Green function series (22) *with j even (resp. j odd) converges with an algebraically small error of order $(j-1)/2$ (resp. $j/2$) to the normal derivative of the function G_j.*

Proof. The proof follows easily from Lemmas 4.2 and 4.3. ☐

4.4 $\tilde{G}^{\mathrm{q}}_j$ nullspace and complete rapidly-convergent Green functions series G^{q}_j

As discussed in the subsection 2.3, it is natural to seek scattered fields $u^s_{\mathcal{D}}$ (for the Dirichlet problem) and $u^s_{\mathcal{N}}$ (Neumann problem) of the form

$$u^s_{\mathcal{D}}(x,y) = \int_{\Gamma_\#} \frac{\partial \tilde{G}^{\mathrm{q}}_j}{\partial\nu(x')}\left(x-x', y-f(x')\right)\,\mu(x')\,ds(\Gamma_\#),$$

$$u^s_{\mathcal{N}}(x,y) = \int_{\Gamma_\#} \tilde{G}^{\mathrm{q}}_j\left(x-x', y-f(x')\right)\,\mu(x')\,ds(\Gamma_\#), \tag{45}$$

where μ and μ are solutions of the equations

$$\int_{\Gamma_\#} \partial_{\nu(x')}\tilde{G}^{\mathrm{q}}_j\left(x-x', f(x)-f(x')\right)\,\mu(x')\;ds(x') + \frac{1}{2}\mu(x') = -u^{\mathrm{inc}}{}_{|\Gamma_\#}, \tag{46}$$

$$\int_{\Gamma_\#} \partial_{\nu(x)}\tilde{G}^{\mathrm{q}}_j\left(x-x', f(x)-f(x')\right)\,\mu(x')\;ds(x') - \frac{1}{2}\mu(x') = -\partial_{\nu(x)}u^{\mathrm{inc}}{}_{|\Gamma_\#}. \tag{47}$$

Remark 4.5. Here and in what follows we assume that

$$h > h_0 = \max_{x\in\left(-\frac{L}{2},\frac{L}{2}\right)} f(x) - \min_{x\in\left(-\frac{L}{2},\frac{L}{2}\right)} f(x). \tag{48}$$

in order to avoid singularities at the points

$$x = x' + nL \quad \text{and} \quad f(x)-f(x') = -\ell h, \quad n\in\mathbb{Z},\;\; \ell\in\mathbb{N}_0,\;\; 0\leq\ell\leq j.$$

As we will see, 1) Equations (46) and (47) are non-invertible at Wood anomalies, and 2) They can fail to be invertible even away from Wood anomalies unless restrictions on the shift parameter h additional to those put forth in Remark (48) are imposed. Roughly speaking, the difficulties 1) and 2) arise from the fact that the quasi-periodic Green function $\tilde{G}^{\mathrm{q}}_j$ fails to include a finite number of Rayleigh modes for certain combinations of the the shift parameter h and the parameters k, θ, L of the scattering problem, as shown in what follows.

In view of equations (14), (22) and (30), away from Wood anomalies we have

$$\tilde{G}_j^{\mathrm{q}}(X,Y) = \sum_{n\in\mathbb{Z}} \frac{i}{2L\beta_n}\left(\sum_{m=0}^{j}(-1)^m C_j^m e^{i\beta_n mh}\right) e^{i\alpha_n X} e^{i\beta_n Y}, \tag{49}$$

so that, for values of h for which

$$\sum_{m=0}^{j}(-1)^m C_j^m e^{i\beta_{n_0} mh} = (1-e^{i\beta_{n_0}h})^j = 0, \tag{50}$$

the Green function $\tilde{G}_j^{\mathrm{q}}(X,Y)$ does not contain the Rayleigh mode $e^{i\alpha_n X}$. In such cases, equations (46) and (47) could be singular— that is, they could admit non-zero solutions for zero right-hand-sides. For instance, for the flat case ($f = 0$), $e^{i\alpha_n x}$ is a non-trivial solution of the Dirichlet integral equation (46); Figure **??**, further, demonstrates the singularity of the problem for cases for which $f \neq 0$. Note that equation (50) can only hold for propagative modes ($n_0 \in U$) and, in particular, there can only be a finite number of values of n for which a resonance of type (50) may occur.

Similar resonance conditions and associated non-uniqueness issues occur at Wood anomalies. To demonstrate this, displaying explicitly the (k,θ) dependence of α_n and β_n by $\alpha_n = \alpha_n(k,\theta)$ and $\beta_n = \beta_n(k,\theta)$, respectively, assume at first that for a given frequency $k = k^0$ and a given incidence angle $\theta = \theta^0$ there is one and only one value of $n \in \mathbb{Z}$, namely $n = n^0$, for which $\beta^n(k^0,\theta^0)$ vanishes: $\beta_{n_0}(k^0,\theta^0) = 0$ and $\beta_n(k^0,\theta^0) \neq 0$ for $n \neq n_0$. Then, it is easy to check that, as (k,θ) approach (k^0,θ^0), the limit of the expansion (49) for G_j^{q} is given by

$$\tilde{G}_j^{\mathrm{q}}(X,Y) = \sum_{n\in\mathbb{Z},n\neq n^0} \frac{i}{2L\beta_n(k^0,\theta^0)}\left(\sum_{m=0}^{j}(-1)^m C_j^m e^{i\beta_n(k^0,\theta^0)mh}\right) e^{i\alpha_n(k^0,\theta^0)X} e^{i\beta_n(k^0,\theta^0)Y}$$
$$+ \lim_{\beta\to 0}\frac{i}{2L\beta}\left(\sum_{m=0}^{j}(-1)^m C_j^m e^{i\beta mh}\right) e^{i\alpha_n(k^0,\theta^0)X} e^{i\beta Y}.$$

But, using a Taylor expansion of $e^{i\beta mh}$ together with the relation (28) at $Z = 0$ it is easily seen that, for $j \geq 2$ we have

$$\lim_{\beta\to 0}\frac{i}{2L\beta}\left(\sum_{m=0}^{j}(-1)^m C_j^m e^{i\beta mh}\right) = 0,$$

and, thus, at the Wood anomaly $\tilde{G}_j^{\mathrm{q}}$ does not contain the Rayleigh mode $e^{i\alpha(k^0,\theta^0)X}$. In this case, again, (46) and (47) can have non-trivial solutions.

Remark 4.6. Note that the non-uniqueness problem at Wood anomalies (which occurs for $j \geq 2$ but not for $j = 1$) arises for all $h > h_0$, and, thus, it is in some sense more fundamental that the non-uniqueness issue arising from resonant-shift condition (50)—which could be bypassed by adequate selection of the somewhat arbitrary shift parameter h. In any case, the two non-uniqueness issues discussed in this section translate, in practice, into ill-posed numerical solvers at and around Wood Anomalies and for shift values in a neighborhood of each resonant shift.

To overcome these difficulties we introduce slightly modified Green functions and correspoding integral equations. The modified Green functions is obtained by simply adding a multiple of each one of the missing modes of the form $e^{i\alpha_n X + i\beta_n Y}$, as discussed in what follows. Clearly, such a procedure results in new outgoing Green functions, since the individual modes added are themselves outgoing solutions of the Helmholtz equation (4)) in the domain Ω. In particular, our algorithm does not resort to selection of non-resonant shift parameters (cf. Remark 4.6).

To address the non-uniqueness issues arising from the resonance condition (50) we proceed as follows: letting $\varepsilon > 0$ and

$$U_{\mathrm{res}}^{\varepsilon} = \{n \in U \ \text{ such that } |h - 2\pi q/\beta_n| < \varepsilon \ \text{ for some integer } q\}\,. \tag{51}$$

we define a smooth Kernel M_{res} by

$$M_{\mathrm{res}}(X,Y) = \sum_{n \in U_{\mathrm{res}}} e^{i\alpha_n X + i\beta_n Y}, \quad X \in (-L, L),\ Y \in \mathbb{R}, \tag{52}$$

and we replace $\tilde{G}_j^{\mathrm{q}}$ in equations (46) and (47) by $\tilde{G}_j^{\mathrm{q}} + M_{\mathrm{res}}$. Similarly, to regularize the integral equations (46) and (47) at Wood anomalies, for $\varepsilon > 0$ we define

$$U_{\mathrm{wa}}^{\varepsilon} = \{n \in \mathbb{Z}, \text{such that } |\beta_n| \le \varepsilon\} \tag{53}$$

and, for any $n \in U_{\mathrm{wa}}^{\varepsilon}$

$$c_n = \max_{x \in (-\frac{L}{2}, \frac{L}{2})} |i\alpha_n f'(x) - i\beta_n|. \tag{54}$$

Then, noting that c_n is necessarily non-zero unless f' vanishes identically, for non-constant f we consider the smooth kernel M_{wa},

$$M_{\mathrm{wa}}(X,Y) = \sum_{n \in U_{\mathrm{wa}}^{\varepsilon}} \frac{e^{i\alpha_n X + i\beta_n Y}}{c_n}, \quad X \in (-L, L),\ Y \in \mathbb{R}. \tag{55}$$

Remark 4.7. For the flat case (constant f) at Wood anomalies we have $c_n = 0$ for some n, and thus M_{wa} is not defined. The kernels $\partial_{\nu(x')} M_{\mathrm{wa}}$ and $\partial_{\nu(x)} M_{\mathrm{wa}}$ can nevertheless be extended to such cases using a limiting process. Indeed for $f' = 0$ we have $c_n = |\beta_n|$, and thus

$$\lim_{\beta_n \to 0} \partial_{\nu(x')} \left\{ \frac{e^{i\alpha_n(x-x') + i\beta_n(y-y')}}{|\beta_n|} \right\} = -ie^{i\alpha_n(x-x')} \lim_{\beta_n \to 0} \frac{\beta_n}{|\beta_n|}$$

Noting that $\lim_{\beta_n \to 0} \frac{\beta_n}{|\beta_n|}$ equals either 1 or i (depending on the sign of $(k^2 - \alpha_n^2)$ as the Wood anomaly is approached), for the flat case at Wood anomalies we replace $\partial_{\nu(x')} M_{\mathrm{wa}}(x - x', y - y')$ and $\partial_{\nu(x)} M_{\mathrm{wa}}(x - x', y - y')$ by one of the two possible associated limits, say,

$$\left\{\partial_{\nu(x')} M_{\mathrm{wa}}\right\}(x - x', y - 0) \to -i \sum_{n \in U_{\mathrm{wa}}^{\varepsilon}} e^{i\alpha_n(x-x')} \quad \text{and} \tag{56}$$

$$\left\{\partial_{\nu(x)} M_{\mathrm{wa}}\right\}(x - x', y - 0) \to i \sum_{n \in U_{\mathrm{wa}}^{\varepsilon}} e^{i\alpha_n(x-x')}. \tag{57}$$

These alternative definitions for the flat case at Wood anomalies (or, indeed, any definition as a sum of arbitrary non-zero multiples of all exponentials $e^{i\alpha_n(x-x')}$ for $n \in U_{\mathrm{wa}}$) do not change the solution for the flat-interface Wood-anomaly case, and lead to solutions that vary continuously as the flat-interface Wood-anomaly case is approached—as long as, as is generally found in applications, the right-hand-side of the integral equation is orthogonal to $e^{i\alpha_n x}$ for all $n \in U_{\mathrm{wa}}^{\varepsilon}$).

Using these additional kernels we can now define a periodic Green function for all smooth periodic interfaces, all incidence angles and all frequencies, namely

$$G_j^{\mathrm{q}}(X,Y) = \tilde{G}_j^{\mathrm{q}}(X,Y) + M_{\mathrm{res}}(X,Y) \quad \text{for the flat-interface Wood-anomaly case, and} \tag{58}$$

$$G_j^{\mathrm{q}}(X,Y) = \tilde{G}_j^{\mathrm{q}}(X,Y) + M_{\mathrm{res}}(X,Y) + M_{\mathrm{wa}}(X,Y), \quad \text{otherwise} \tag{59}$$

(with the substitutions (56) and (57) when appropriate, as indicated in Remark 4.7), our second kind integral equations for the Dirichlet and Neumann are given by

$$\frac{1}{2}\mu(x) + \int_{\Gamma_\#} \left\{\partial_{\nu(x')} G_j^{\mathrm{q}}\right\}(x-x', f(x)-f(x'))\mu(x')\, ds(x') = -u^{\mathrm{inc}}{}_{|\Gamma_\#} \quad \text{and} \tag{60}$$

$$-\frac{1}{2}\mu(x) + \int_{\Gamma_\#} \left\{\partial_{\nu(x)} G_j^{\mathrm{q}}\right\}(x-x', f(x)-f(x'))\mu(x')\, ds(x') = -\partial_{\nu(x)} u^{\mathrm{inc}}{}_{|\Gamma_\#}. \tag{61}$$

The Dirichlet and Neumann scattering problems under consideration thus reduce to finding $\mu \in \mathcal{C}^\alpha_\#(\Gamma_\#)$ and $\mu \in \mathcal{C}^\alpha_\#(\Gamma_\#)$ such that equations (60) and (61) are satisfied, where $\mathcal{C}^\alpha_\#(\Gamma_\#)$ denotes the space of continuous α-quasi-periodic functions.

Reference [] provides proofs of existence and uniqueness for these problems on the basis of corresponding results for the associated PDEs. Numerical algorithms for these problems and numerical results illustrating these methods are presented in the following two sections.

5 Numerical algorithm

Our numerical method for the solution of equations (60) and (61) incorporates the windowing and shifting methodologies developed in Sections 3 and 4 for evaluation of invertible integral operators at all frequencies together with a suitable modified version of a well known Nyström approach for high-order evaluation of logarithmic integral operators. This section presents the details of a numerical implementation of the combined windowing-shifting based Nyström approach.

5.1 Periodic setting and kernel decomposition

The Nyström approach [2, 27–29] relies on decomposition of the integral kernel as a sum of a smooth kernel and a logarithmic term. We present our decomposition for the Dirichlet equation (60); the method for Neumann equation (61) is entirely analogous. Using the change of unknown $\tilde{\mu}(x) = \mu(x)e^{-i\alpha x}$ we re-express the integral on the left-hand side of equation (60) in the form

$$\int_{-\frac{L}{2}}^{\frac{L}{2}} \left\{\partial_{\nu(x')} G_j^{\mathrm{q}}\right\}(x-x', f(x)-f(x'))\, \phi(x,x')\, \tilde{\mu}(x') \sqrt{1+f'(x')^2}\, dx' + \frac{1}{2}\tilde{\mu} = -u^{\mathrm{inc}}{}_{|\Gamma_\#} e^{-i\alpha x}, \tag{62}$$

where $\tilde{\mu}$ is a periodic function of period L and where $\phi(x,x') = e^{i\alpha(x-x')}$. In view of (58) and (59) and expressing the integral involving the periodic Green function $\tilde{G}_j^{\mathrm{q}}$ as an integral between $-\infty$ and ∞ (cf. equation (19)) where the corresponding identity for the kernel $\tilde{G}^{\mathrm{q}}$ is displayed) the integral on the left-hand side of (62) can be expressed in the form

$$\int_{-\frac{L}{2}}^{\frac{L}{2}} \partial_{\nu(x')} \left\{M_{\mathrm{res}} + M_{\mathrm{wa}}\right\}(x-x', f(x)-f(x'))\, \phi(x,x')\, \tilde{\mu}(x')\, \sqrt{1+f'(x')^2}\, dx' +$$
$$\int_{-\infty}^{+\infty} \left\{\partial_{\nu(x')} G_j\right\}(x-x', f(x)-f(x'))\, \phi(x,x')\, \tilde{\mu}(x')\, \sqrt{1+f'(x')^2}\, dx'. \tag{63}$$

The first term in (63) is smooth and periodic, and therefore, the associated integral operator can be computed with high-order accuracy by means of the trapezoidal rule. To evaluate the second term in (63), in turn, we first truncate the integral using the windowing methodology introduced in Section 3, that is we approximate the second integral (63) by

$$\int_{-\infty}^{+\infty} S(x-x', cA, A)\, \partial_{\nu(x')} G_j(x-x', f(x)-f(x'))\, \phi(x,x')\, \tilde{\mu}(x')\, \sqrt{1+f'(x')^2}\, dx' \tag{64}$$

for adequately selected positive constants c and A, and we then evaluate the integral (64), with high-order accuracy, by accounting explicitly for the logarithmic singularity at the origin. To do this we follow [2, p. number] and note that, for $|x-x'| \leq 2\pi$, the kernel $\partial_{\nu(x')} G_j$ can be expressed in the form

$$\partial_{\nu(x')} G_j(x-x', f(x)-f(x')) = K_1(x,x') \ln\left[4\sin^2\left(\frac{x-x'}{2}\right)\right] + K_2(x,x'), \tag{65}$$

where

$$K_1(x,x') = \frac{k}{4\pi} \frac{f(x')(x-x') - (f(x')-f(x))}{\sqrt{1+f'(x')^2}} \frac{J_1\left(k\sqrt{(x-x')^2+(f(x)-f(x'))^2}\right)}{\sqrt{(x-x')^2+(f(x)-f(x'))^2}},$$

and

$$K_2(x,x') = \partial_{\nu(x')} G_j(x-x', f(x)-f(x')) - K_1(x,x') \ln\left[4\sin^2\left(\frac{x-x'}{2}\right)\right],$$

are smooth functions.

In the context [2, p. number] the condition $|x-x'| \leq 2\pi$ is always satisfied; unfortunately, however, this is not the case for the integration problem (64): under the present conditions, use of the decomposition for which $-\infty < x-x' < \infty$, would lead to singularities whenever $x-x'$ is an integer multiple of 2π. To overcome this difficulty we utilize an additional cut-off function that vanishes outside a sufficiently small neigborhood of the singular point $x'=x$: taking $0 < A_\mathrm{s} < L/2$ and $0 < c_s < 1$ we define the windowing function

$$P_\mathrm{s}(x-x', c_\mathrm{s}, A_\mathrm{s}) = S(x-x', c_\mathrm{s}A_\mathrm{s}, A_\mathrm{s}), \quad c_\mathrm{s}\ ,\ A_\mathrm{s} \in \mathbb{R}_{>0}, \tag{66}$$

and we decompose the integrand in (64) in the form

$$\begin{aligned} S(x-x', cA, A)\left\{\partial_{\nu(x')} G_j^{\mathrm{q}}\right\}(x-x', f(x)-f(x'))\, \phi(x,x')\, \sqrt{1+f'(x')^2} = \\ K_\mathrm{s}(x,x') \ln\left[4\sin^2\left(\frac{\pi}{L}(x-x')\right)\right] + K_\mathrm{r}(x,x') \end{aligned} \tag{67}$$

where

$$\begin{aligned} K_\mathrm{s}(x,x') = \frac{k}{4\pi}\, P_\mathrm{s}(x-x', c_\mathrm{s}, A_\mathrm{s})\, \frac{f(x')(x-x') - (f(x')-f(x))}{\sqrt{(x-x')^2+(f(x)-f(x'))^2}} \\ J_1\left(k\sqrt{(x-x')^2+(f(x)-f(x'))^2}\right), \end{aligned} \tag{68}$$

and

$$\begin{aligned} K_\mathrm{r}(x,x') = S(x-x', cA, A)\left\{\partial_{\nu(x')} G_j^{\mathrm{q}}\right\}(x-x', f(x)-f(x'))\, \phi(x,x')\, \sqrt{1+f'(x')^2} \\ - K_\mathrm{s}(x,x') \ln\left[4\sin^2\left(\frac{\pi}{L}(x-x')\right)\right]. \end{aligned} \tag{69}$$

It is easy to check that, given the assumptions $0 < A_\mathrm{s} < L/2$ and $0 < c_\mathrm{s} < 1$, K_s and K_r are smooth functions of x and x', and, thus, the MK methodology [27, 28] can be used for evaluation of the integral (63)—as detailed in the following section.

5.1.1 MK quadrature rules

To derive MK quadrature rules in the present context, we use the decomposition (67) to re-express the integral (63) in the form

$$\int_{-\frac{L}{2}}^{\frac{L}{2}} \partial_{\nu(x')} K_\mathrm{r}^\mathrm{per}(x,x')\tilde{\mu}(x')\ dx' + \\ \int_{-\infty}^{+\infty} K_\mathrm{r}(x,x')\tilde{\mu}(x')\,dx' + \int_{-\infty}^{+\infty} K_\mathrm{s}(x,x')\ln\left[4\sin^2\left(\frac{\pi}{L}(x-x')\right)\right]\tilde{\mu}(x'),)\,dx' \quad (70)$$

where $K_\mathrm{r}^\mathrm{per}(x,x') = \partial_{\nu(x')}\left\{M_\mathrm{res}+M_\mathrm{wa}\right\}(x-x', f(x)-f(x'))\,\phi(x,x')\sqrt{1+f'(x')^2}$. Additionally we use an equispaced discretization of the integration domain containing an even number n_i of points per period of the scattering surface: denoting by $n_{per} = \lceil \frac{A}{L} \rceil$ the number of periodic intervals contained in the integration domain to the right of the point $x = \frac{L}{2}$ (where $\lceil x \rceil$ denotes the smallest integer larger than or equal to x), the quadrature rule uses a total of $(2n_{per}+1)n_i$ quadrature points x_j given by

$$x_j = (-\frac{L}{2} - n_{per}L) + (j-1)\frac{L}{n_i}, \qquad j \in \mathbb{N}, \quad j \leq (2n_{per}+1)n_i,$$

over an integration domain consisting of $2n_{per}+1$ periodic intervals.

Our MK quadrature rule then results as follows: The first integral in equation (70) is evaluated with high-order accuracy by means of the trapezoidal rule formula

$$\int_{-\frac{L}{2}}^{\frac{L}{2}} K_\mathrm{add}(x,x')\,\tilde{\mu}(x')\ dx' \approx \frac{L}{n_i}\sum_{-\frac{L}{2}\leq|x-x_j|\leq\frac{L}{2}} K_\mathrm{add}(x,x_j)\,\tilde{\mu}(x_j). \quad (71)$$

Similarly, the second term in (70) is integrated with high-order accuracy by means of the trapezoidal rule expression

$$\int_{-\infty}^{+\infty} K_\mathrm{r}(x',x)\tilde{\mu}(x')dx' \approx \frac{L}{n_i}\sum_{|x-x_j|\leq A} K_\mathrm{r}(x,x_j)\,\tilde{\mu}(x_j). \quad (72)$$

Finally, the third term in (70) (the singular integral) is approximated by means of the MK quadrature rule

$$\int_{-\infty}^{+\infty} K_\mathrm{s}(x,x')\ln\left[4\sin^2\left(\frac{\pi}{L}(x-x')\right)\right]\ \tilde{\mu}(x')dx' \\ = \int_{x-\frac{L}{2}}^{x+\frac{L}{2}} K_\mathrm{s}(x',x)\ln\left[4\sin^2\left(\frac{\pi}{L}(x-x')\right)\right]\ \tilde{\mu}(x')dx' \\ \approx \frac{L}{2\pi}\sum_{|x-x_j|\leq A_\mathrm{s}} \mathcal{R}_{j,n_i}\left(\frac{2\pi x}{L}\right) K_\mathrm{s}(x,x_j)\,\tilde{\mu}(x_j), \quad (73)$$

where

$$\mathcal{R}_{j,n_i}(t) = \frac{1}{n_i}\sum_{q=-\frac{n_i}{2}+1}^{\frac{n_i}{2}} \int_0^{2\pi} e^{iq(\frac{2\pi x_j}{L}+\tau-t)}\ln\left(4\sin^2\frac{\tau}{2}\right)d\tau. \quad (74)$$

Formula (73) is obtained by introducing the change of variables $t = \frac{2\pi}{L}x$, $\tau = \frac{2\pi}{L}x'$ and expressing $K_{\mathrm{s}}(x,x')\,\tilde{\mu}(x')$ as a Fourier series. Using the relation [3, ch. 12]

$$\frac{1}{2\pi}\int_0^{2\pi} \ln\left(4\sin^2\frac{\tau}{2}\right) e^{im\tau} d\tau = \begin{cases} 0 & \text{if } m = 0 \\ -\dfrac{1}{m} & m = 1, 2, \cdots \end{cases}$$

we obtain

$$\mathcal{R}_{j,n_i}\left(\frac{2\pi\, x_i}{L}\right) = -\frac{4\pi}{n_i}\left[\sum_{q=1}^{\frac{n_i}{2}} \frac{1}{|q|}\cos\left(q\left(\frac{2\pi}{L}(x_i - x_j)\right)\right)\right] - \frac{4\pi}{n_i^2}\cos\left(\frac{n_i}{2}\left(\frac{2\pi}{L}(x_i - x_j)\right)\right) \tag{75}$$

and our MK quadrature rule for the integral (70) is complete.

6 Numerical results

This section presents a variety of numerical results demonstrating the properties of the rapidly convergent Green function (Section 6.1) and associated rough-surface scattering solvers (Sections 6.2 through 6.4). These results demonstrate the applicability and efficiency of the overall methodology throughout the spectrum, including frequencies at and around Wood anomalies. For definiteness, throughout this section we consider problems of scattering by two profiles, including the sinusoidal profile

$$f_1(x) = \frac{H}{2}\cos(\frac{2\pi x}{L}) \tag{76}$$

for various values of h, as well as the multi-frequency profile given in equation (78). We demonstrate our solvers for a range of frequencies and incidence angles varying from normal incidence ($\theta = 0$) to near grazing incidence ($\theta = \pi/2$).

6.1 Convergence rate of the quasi-periodic Green function for various differencing orders

Figures 2 and 3 display the absolute error in the rapidly convergent Green functions of various d-orders for two frequencies, namely, non-Wood anomaly frequency $k = 1.5$ and the Wood anomaly frequency $k = 1$. The left portions of these figures present results that arise as direct differencing is used for all values of N; a reduction in the convergence rates for large values of N, which results from cancellation errors in the differencing process, is clearly discernible in both left figures. The two right-hand figures, in turn, display results in which, direct differencing is substituted by the Taylor approximation

$$G_j(X,Y) \approx f_j^{(j)}(0) \approx \sum_{q=0}^{Q} f_j^{(j+q)}(0)\left\{\sum_{l=1}^{j}\frac{C_l^j(-1)^l}{(j+q)!}\left(\frac{l}{j}\right)^{j+q}\right\}. \tag{77}$$

6.2 Effect of regularization terms

To demonstrate the beneficial effect of the corrections introduced in equations (58) and (59) we let $f(x) = \frac{\pi}{10}\cos(x)$ ($L = 2\pi$), and the incident angle $\theta = \pi/9$, for which 4 non-evanescent modes exist: $U = \{-2, 1, 0, 1\}$.

First, as expected, the discrete problem associated with the unregularized integral equation (46) is ill-conditioned for values of h for which the resonance condition (50) holds, namely, values of h at and around

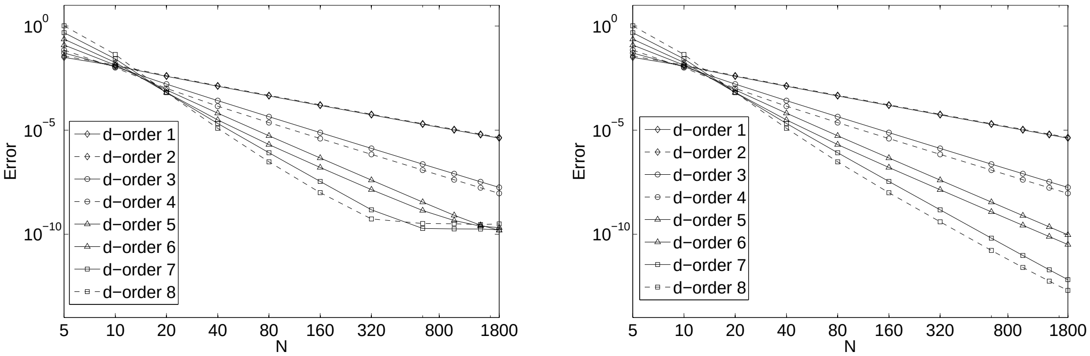

Figure 2: Absolute approximation error arising from the rapidly convergent Green function as a function of the truncation parameter N for various differencing orders j at the frequency $k = 1.5$—which is away from the set of $\{1, 2, 3, \dots\}$ of Wood anomaly frequencies. Left: Direct differencing for all values of n. Right: Taylor differencing for n large enough. Note that, as stated in Theorem 3.1 and demonstrated in Table 3), our use of the windowing function approach embodied in equations 17 and 18 further accelerates convergence, at least away from Wood anomalies, beyond the rates shown in the present table.

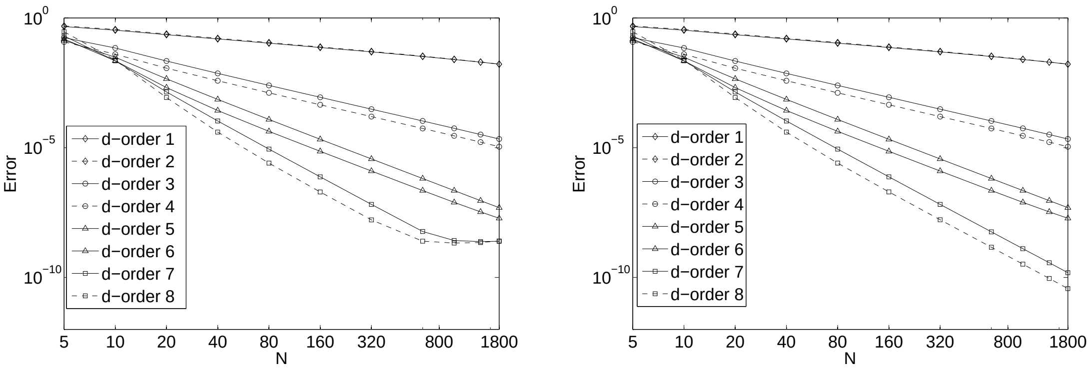

Figure 3: Absolute approximation error arising from the rapidly convergent Green function as a function of the truncation parameter N for various differencing orders j at the Wood anomaly frequency $k = 1$. Left: Direct differencing for all values of n. Right: Taylor differencing for n large enough.

d-order	1	2	3	4	5	6	7	8
c-order for $k = 1.5$ (away from Wood anomalies)	3/2	3/2	5/2	5/2	7/2	7/2	9/2	9/2
c-order at $k = 1$ (Wood anomaly)	1/2	1/2	3/2	3/2	5/2	5/2	7/2	7/2

Table 2: Observed convergence order “c-order” for various finite differencing orders “d-order”, as displayed in Figures 2 and 3 : Note that, for the Wood anomaly case, the observed convergence orders are exactly the ones predicted by the theory.

the set $\mathcal{H} = \left\{ h \in \mathbb{R}^+,\ h = \frac{2\pi q}{\beta_n}, q \in \mathbb{N},\ n \in U \right\}$; for instance, $h_c = \frac{2\pi}{\beta_0} \approx 3,3432$ is a resonance value. In the left part of Figure 4, we display the evolution of the condition number of the matrix associated to both the unregularized (46) and the regularized (60) problems. The experiment is done with the Green function of order 5 ($j = 5$) and a grating of equation $f(x) = \frac{\pi}{10}\cos(x)$. For the unregularized problem, the condition number blows up as h tends to the critical value h_c ; on the contrary, for the regularized problem remains well-posed in the neighborhood of h_c. Of course, the error on the energy balance increases a lot as the condition number blows up (cf . Figure 4, left)

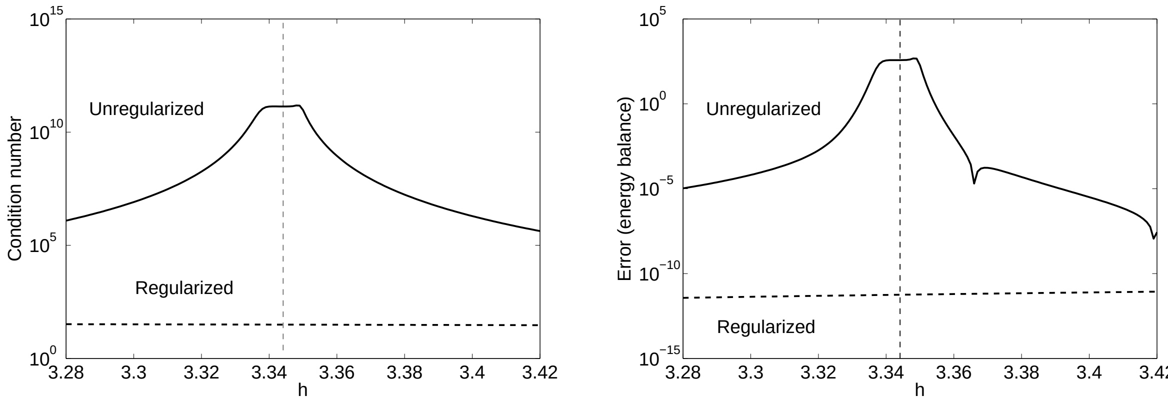

Figure 4: Left : Condition number as a function of the shift parameter h, Right : Energy balance with respect to h

At the Wood anomalies, we also observe ill-conditioning issues for $j \geq 2$ (see Figure 5). We consider the same configuration as previously: we take $L = 2\pi$ and an incident angle $\theta = \pi/9$, $f(x) = \frac{\pi}{10}\cos(x)$, and $h = 2$ (so that condition (50) is not satisfied). The set of Wood anomaly frequencies is then given by $W = \{k \in \mathbb{R}^2, k^2 = (k\sin(\theta) + n)^2, n \in \mathbb{Z}\}$. For instance $k_1 = 1/(1 + \sin(\theta)) \approx 0.74$ is a Wood anomaly. On the left part of figure 5, we display the condition number of the matrix associated to both the unregularized (46) and regularized (60) problems as a function of the frequency k. The experiment is done with the Green function of order 7. Again, the condition number blows up as k tends to the Wood anomalies when using the unregularized problem although the problem remains well-conditionned when solving the regularized one.

Finally, In Figure 6, we plot the evolution of the energy with respect to k for the classical green function (with windowing in blue) and for the 9th order shift green function for a grating of equation . As expected, our new method works also at the Wood anomalies, although the classical method fails.

6.3 Convergence rate of the energy balance and the efficiencies

In a second step, we plot the evolution of the error on the energy balance with respect to A when a grating, we take a grating of equation $f(x) = \frac{2\pi}{10}\cos(x)$. In Figure 6.3, A is going from 50 to 450. As expected, we obtain straight lines of different orders. For the first order, we obtain a slope of $1/2$, for the second and third order, we get a slop of $3/2$, for the 4th and 5th order, we get a slop of $5/2$ and finally for the 6th order we get a slop of $7/2$. We expected this kind of shift in the convergence rate of our model, but, for the energy and for the even orders, we get a better convergence rate as the expected one (which we do not observe on the convergence of the solution of the integral equation itself).

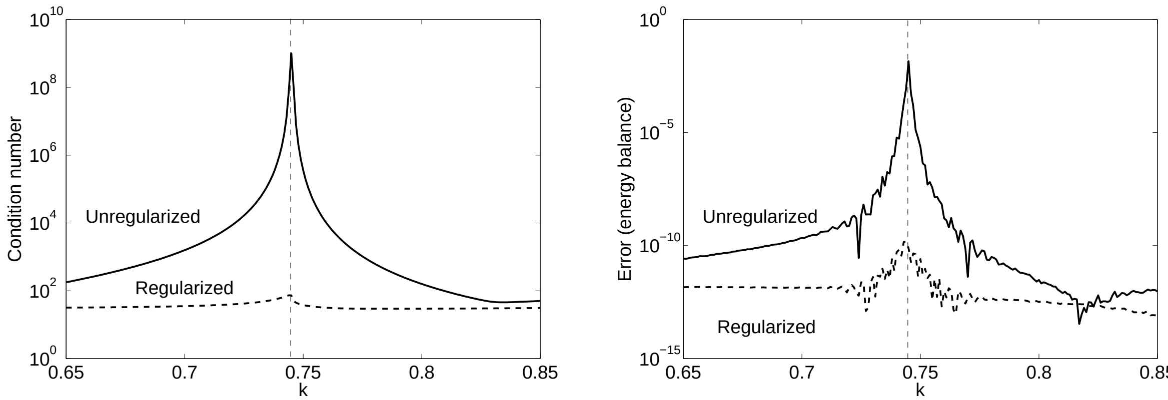

Figure 5: Left: Condition number as a function of the shift parameter k, Right : Energy balance with respect to k

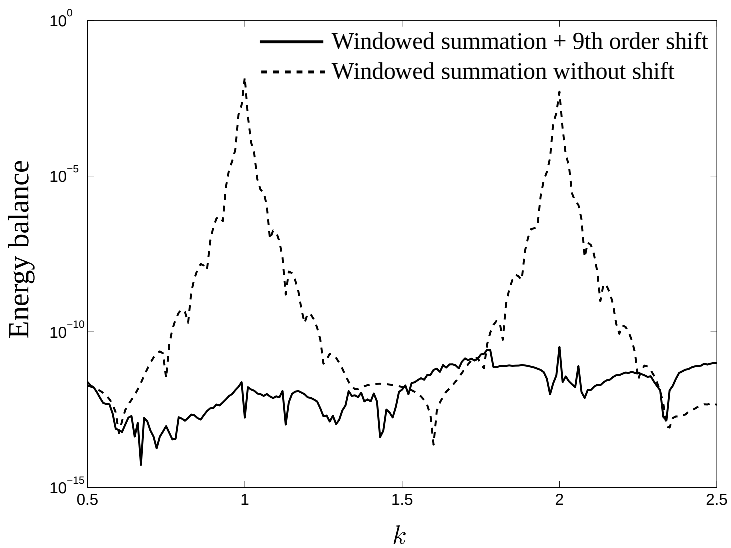

Figure 6: Energy balance with respect to the frequency

6.4 First order bragg configuration

Finaly, we study the behavior of our model in the first order Bragg resonance condition for different gratings (see [30] , [31] and [32]). We remind that the direction of the propagative modes are given by $\alpha_n = \alpha + n\frac{2\pi}{L}$, which can be written in term of diffraction angle:

$$\sin(\theta_n) = \sin(\theta) + n\frac{2\pi}{kL}, n \in \mathbb{Z}$$

The first order Brag configuration corresponds to the case where $\sin(\theta_{-1}) = -\sin(\theta)$, which means that $\frac{2\pi}{kL} = 2\sin(\theta)$. In Figure 9, we plot the energy and the efficiency e_{-1} of the mode -1 with respect to the frequency k for different 2π periodic gratings of equation $f_1(x) = 2\pi\, D\, cosx$, $D \in \{0.1, 0.2, 0.5\}$ (see Figure 8). Wood anomalies values correspond to the dotted lines on the efficiency graph. The deeper the

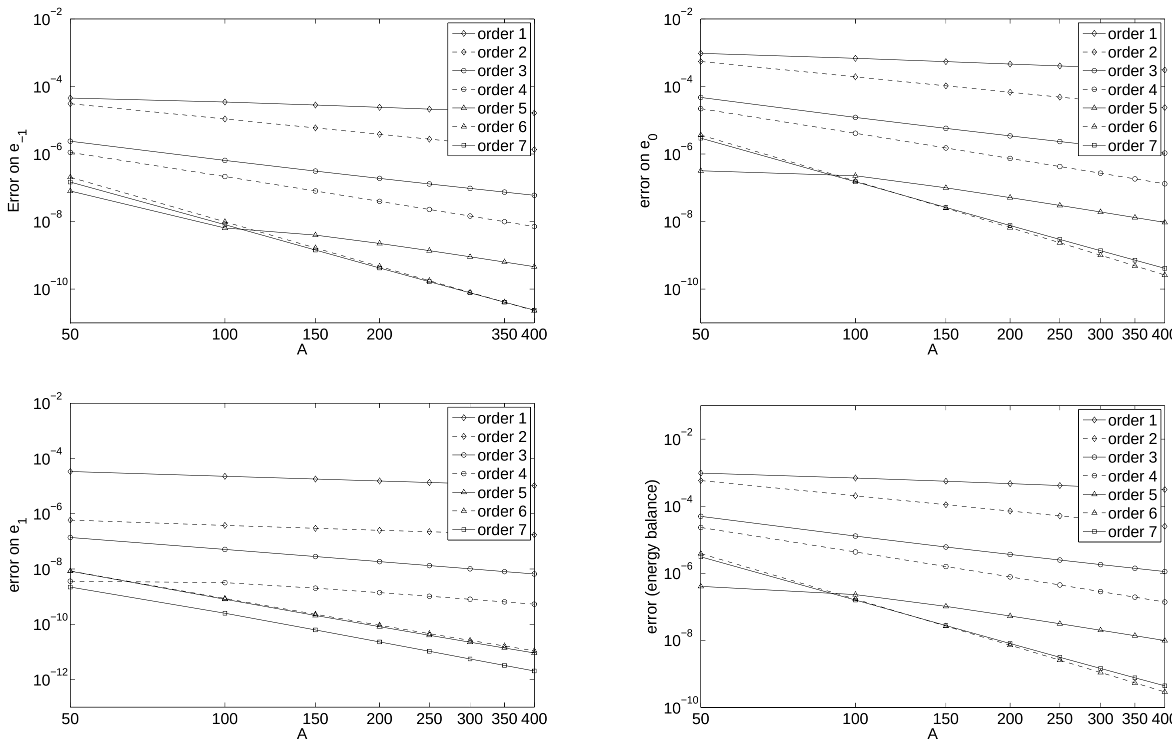

Figure 7: Evolution of the error on the energy with respect to A for different Green functions

grating is the more oscillatory the associated efficiency curve is.

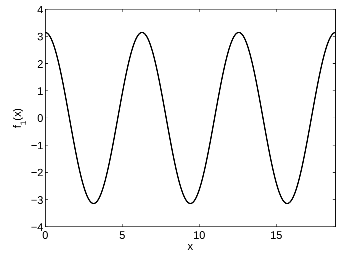

Figure 8: Gratting $f_1(x) = 2\pi\, D\, cos x$ for $D = 0.5$

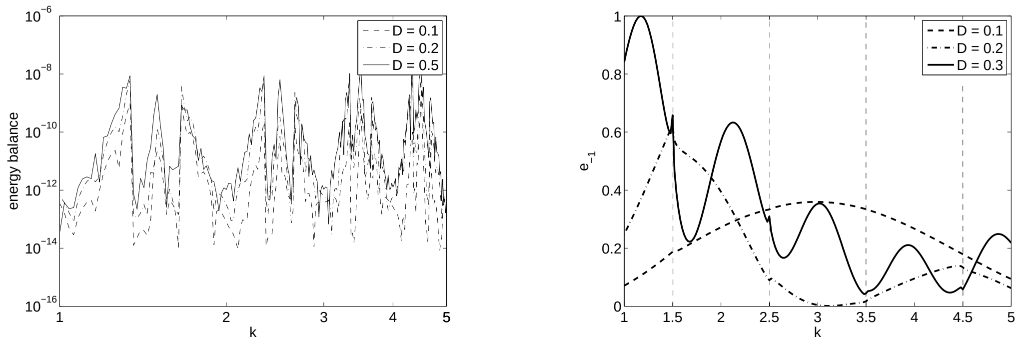

(a) Evolution of the energy

(b) Evolution of the efficiency e_{-1}

Figure 9: Evolution of the energy balance and the efficiency e_1 with respect to k in the first order Bragg configuration

The same experiment is reproduced in Figure 11 for a more complicated family of gratings (see Figure 10)

$$f_2(x) = 2\pi\, D\, (0.4 \cos x - 0.2 \cos(2x) + 0.4 \cos(3x))\,, \quad D \in \{0.1, 0.2, 0.4\}. \tag{78}$$

References

[1] D. Maystre. Rigorous vector theories of diffraction gratings. volume 21 of *Progress in Optics*, pages 1 – 67. Elsevier, 1984.

[2] D. Colton and R. Kress. *Inverse Acoustic And Electromagnetic Scattering Theory*, volume 93 of *Applied Mathematical Sciences*. Springer-Verlag, Berlin, second edition, 1998.

[3] R. Kress. *Linear Integral Equations*, volume 82 of *Applied Mathematical Sciences*. Springer-Verlag, New York, second edition, 1999.

[4] J. DeSanto, G. Erdmann, W. Hereman, and M. Misra. Theoretical And Computational Aspects Of Scattering From Rough Surfaces: One-Dimensional Perfectly Reflecting Surfaces. *Waves In Random Media*, 8(4):385–414, OCT 1998.

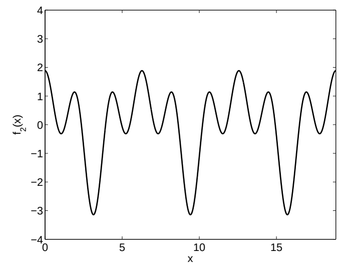

Figure 10: Gratting $f_2(x) = 2\pi\, D\,(0.4\cos x - 0.2\cos(2x) + 0.4\cos(3x))$ for $D = 0.5$

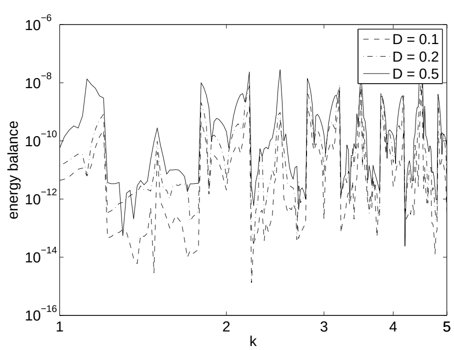

(a) Evolution of the energy

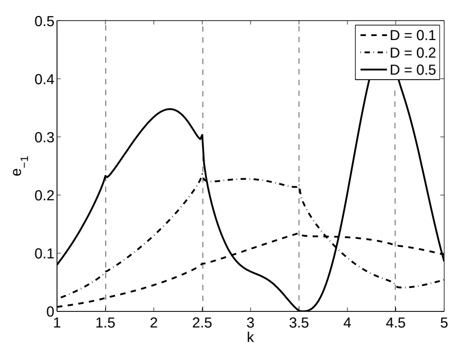

(b) Evolution of the efficiency e_{-1}

Figure 11: Evolution of the energy balance and the efficiency e_1 with respect to k in the first order Bragg configuration

[5] T. Arens, S.N. Chandler-Wilde, and J.A. DeSanto. On Integral Equation And Least Squares Methods For Scattering By Diffraction Gratings. *Communications In Computational Physics*, 1(6):1010–1042, DEC 2006.

[6] O.p. Bruno and F. Reitich. Numerical-Solution Of Diffraction Problems - A Method Of Variation Of Boundaries. *Journal Of The Optical Society Of America A-Optics Image Science And Vision*, 10(6):1168–1175, JUN 1993.

[7] A.W. Mathis and A.F. Peterson. A Comparison Of Acceleration Procedures For The Two-Dimensional Periodic Green's Function. *IEEE Transactions On Antennas And Propagation*, 44(4):567–571, APR 1996.

[8] S.N. Chandler-Wilde and D.C. Hothersall. Efficient calculation of the Green function for acoustic propagation above a homogeneous impedance plane. *J. Sound Vibration*, 180(5):705–724, 1995.

[9] N.A. Nicorovici, R.C. McPhedran, and R. Petit. Efficient Calculation Of The Greens-Function For Electromagnetic Scattering By Gratings. *Physical Review E*, 49(5, Part b):4563–4577, MAY 1994.

[10] C.M. Linton. Lattice Sums For The Helmholtz Equation. *SIAM Review*, 52(4):630–674, 2010.

[11] N.A. Nicorovici and R.C. McPhedran. Lattice Sums For Off-Axis Electromagnetic Scattering By Gratings. *Physical Review E*, 50(4):3143–3160, OCT 1994.

[12] A. Dienstfrey, F. Hang, and J. Huang. Lattice sums and the two-dimensional, periodic green's function for the helmholtz equation. *Proceedings: Mathematical, Physical and Engineering Sciences*, 457(2005):pp. 67–85, 2001.

[13] A. Moroz. Exponentially Convergent Lattice Sums. *Optics Letters*, 26(15):1119–1121, AUG 1 2001.

[14] C.M. Linton. The green's function for the two-dimensional helmholtz equation in periodic domains. *J. Engrg. Math.*, 33(4):377–402, 1998.

[15] F. Capolino, D. R. Wilton, and W. A. Johnson. Efficient computation of the 3d green's function for the helmholtz operator for a linear array of point sources using the ewald method. *J. Comput. Phys.*, 223(1):250–261, 2007.

[16] T. Arens, K. Sandford, S. Schmitt, and A. Lechleichter. Analysing ewald's method for the evaluation of green functions for periodic media. *(submitted) IMA J. Numer. Anal.*, 2010.

[17] Jr. John A. Monro. *A Super-Algebraically Convergent, Windowing-Based Approach to the Evaluation of Scattering from Periodic Rough Surfaces*. PhD thesis, Californian Institute of Technology, 2007.

[18] Bo Zhang and Simon N. Chandler-Wilde. Integral equation methods for scattering by infinite rough surfaces. *Math. Methods Appl. Sci.*, 26(6):463–488, 2003.

[19] S.N. Chandler-Wilde and C.R. Ross. Scattering by rough surfaces: the Dirichlet problem for the Helmholtz equation in a non-locally perturbed half-plane. *Math. Methods Appl. Sci.*, 19(12):959–976, 1996.

[20] A. Barnett and L. Greengard. A new integral representation for quasi-periodic scattering problems in two dimensions. *BIT*, 51(1):67–90, 2011.

[21] A. Barnett and L. Greengard. A new integral representation for quasi-periodic fields and its application to two-dimensional band structure calculations. *J. Comput. Phys.*, 229(19):6898–6914, 2010.

[22] R. Petit, editor. *Electromagnetic Theory Of Gratings*, volume 22 of *Topics in Current Physics*. Springer-Verlag, Berlin, 1980.

[23] A. Kirsch. Diffraction by periodic structures. In *Inverse problems in mathematical physics (Saariselkä, 1992)*, volume 422 of *Lecture Notes in Phys.*, pages 87–102. Springer, Berlin, 1993.

[24] Anne-Sophie Bonnet-Bendhia and Felipe Starling. Guided waves by electromagnetic gratings and nonuniqueness examples for the diffraction problem. *Math. Methods Appl. Sci.*, 17(5):305–338, 1994.

[25] J.-C. Nédélec and F. Starling. Integral equation methods in a quasi-periodic diffraction problem for the time-harmonic Maxwell's equations. *SIAM J. Math. Anal.*, 22(6):1679–1701, 1991.

[26] N.N. Lebedev. *Special Functions And Their Applications*. Revised English edition. Translated and edited by Richard A. Silverman. Prentice-Hall Inc., Englewood Cliffs, N.J., 1965.

[27] R. Kussmaul. Ein numerisches verfahren zur lösung des neumannschen außenraumproblems für die helmholtzsche schwingungsgleichung. *Computing*, 4:246–273, 1969. 10.1007/BF02234773.

[28] Erich Martensen. Über eine methode zum räumlichen neumannschen problem mit einer anwendung für torusartige berandungen. *Acta Mathematica*, 109:75–135, 1963. 10.1007/BF02391810.

[29] E. Nyström. Über die praktische auflösung von integralgleichungen mit anwendungen auf randwertaufgaben. *Acta Mathematica*, 54:185–204, 1930. 10.1007/BF02547521.

[30] A Sei, O Bruno, and M Caponi. Study of polarization dependent scattering anomalies with application to oceanic scattering. *Radio Science*, 34(2):385–411, MAR-APR 1999.

[31] Oscar P. Bruno and Michael C. Haslam. Efficient high-order evaluation of scattering by periodic surfaces: deep gratings, high frequencies, and glancing incidences. *J. Opt. Soc. Amer. A*, 26(3):658–668, 2009.

[32] Oscar P. Bruno and Michael C. Haslam. Efficient high-order evaluation of scattering by periodic surfaces: vector-parametric gratings and geometric singularities. *Waves Random Complex Media*, 20(4):530–550, 2010.